Title

Optogenetic perturbation of preBötzinger complex inhibitory neurons modulates respiratory pattern

Journal

Nature Neuroscience, 18(3)

ISSN

1097-6256

Authors

Sherman, David
Worrell, Jason W
Cui, Yan
et al.

Publication Date

2015-03-01

DOI

10.1038/nn.3938

Peer reviewed

nature neuroscience

Optogenetic perturbation of preBötzinger complex inhibitory neurons modulates respiratory pattern

David Sherman[1], Jason W Worrell[1], Yan Cui[1,2] & Jack L Feldman[1]

Inhibitory neurons make up a substantial fraction of the neurons in the preBötzinger complex (preBötC), a site that is critical for mammalian eupneic breathing. We investigated the role of glycinergic preBötC neurons in respiratory rhythmogenesis in mice using optogenetically targeted excitation and inhibition. Channelrhodopsin-2 (ChR2) or Archaerhodopsin (Arch) were expressed in glycinergic preBötC neurons of glycine transporter 2 (*Glyt2*, also known as *Slc6a5*)-*Cre* mice. In ChR2-transfected mice, brief inspiratory-phase bilateral photostimulation targeting the preBötC prematurely terminated inspiration, whereas expiratory-phase photostimulation delayed the onset of the next inspiration. Prolonged photostimulation produced apneas lasting as long as the light pulse. Inspiratory-phase photoinhibition in Arch-transfected mice during inspiration increased tidal volume without altering inspiratory duration, whereas expiratory-phase photoinhibition shortened the latency until the next inspiration. During persistent apneas, prolonged photoinhibition restored rhythmic breathing. We conclude that glycinergic preBötC neurons modulate inspiratory pattern and are important for reflex apneas, but that the rhythm can persist after substantial dampening of their activity.

Breathing in mammals is a complex behavior that must work (nearly) continuously throughout life and can be rapidly modified, even transiently stopped, to support a wide range of physiological and functional demands. The preBötC, in the ventrolateral medulla, is a critical locus for respiratory rhythmogenesis in the intact eupneic mammal[1] and in reduced rodent *en bloc* and slice preparations[2]. The preBötC contains intermingled heterogeneous populations of excitatory and inhibitory neurons[3,4]. Excitatory preBötC neurons are critical components of the respiratory central pattern generator (CPG)[1,5–7]. However, the role of inhibitory preBötC neurons is not well understood. Although strong inhibitory currents are observed in intracellular recordings of presumptive preBötC neurons in deeply anesthetized adult cats and rodents[8,9], respiratory rhythm persists after bilateral blockade of fast inhibitory neurotransmission in the preBötC in anesthetized spontaneously breathing adult rats[10]. Given that there is a substantial population of glycinergic preBötC neurons[3], some of which are phasically active during inspiration[11], we wanted to determine their contribution to breathing movements by examining the effects of rapid, acute perturbations of their ongoing activity *in vivo*.

We used optogenetic tools to probe the functional contribution of glycinergic preBötC neurons to respiratory rhythm and pattern. We used viral transfection to express ChR2 or Arch in glycinergic preBötC neurons by locally injecting Cre recombinase–dependent viruses into the preBötC of transgenic mice expressing Cre driven by the *Glyt2* promoter[12–14]. Given that the *Glyt2* promoter is specific to glycinergic neurons[15], this intersectional strategy allowed us to selectively activate and silence these inhibitory neurons in intact, awake or anesthetized, spontaneously breathing mice. We found that perturbing glycinergic neuronal activity in the preBötC profoundly modulated the amplitude and timing of inspiratory motor output and expiratory period with no indications that they were critical for rhythmogenesis.

RESULTS

Targeting opsin expression to preBötC GlyT2 neurons

To express ChR2 or Arch in glycinergic preBötC neurons, we used adeno-associated viruses (AAV 2/1) encoding either *ChR2-eYFP* driven by the constitutive promoter *Ef1α* in a double *loxP*-flanked inverted open reading frame configuration (DIO-ChR2)[16] or *Arch-GFP* driven by the constitutive chicken β-actin (*CBA*) promoter in a FLEX switch (FLEX-Arch). We injected either virus bilaterally into the preBötC of transgenic mice expressing Cre recombinase under the *Glyt2* promoter (**Fig. 1a**,**b**). These injections produced protein expression in preBötC neurons that was detectable *post hoc*, with some expression in neighboring neurons outside of the preBötC, including in the ventral respiratory column (VRC) in the rostral-caudal direction, particularly caudal to the preBötC (**Fig. 1a–d**). We found no evidence of transfected neurons at more distant brainstem sites, including those with established projections to preBötC, such as nucleus of the solitary tract (NTS) and parabrachial nucleus. The peak density of transfected neurons was caudal to the facial nucleus (VII) by 750–900 μm in ChR2-transfected mice and 600–750 μm in Arch-transfected mice and ventral to the compact nucleus ambiguus, which predominately overlapped with the rostrocaudal distribution of somatostatin (*Sst*)-expressing glutamatergic neurons[1,4] (**Fig. 1c**,**d**) that demark the preBötC[4]. In the preBötC, transfected neurons intermingled, but rarely colocalized, with *Sst* immunoreactivity in mice transfected with either DIO-ChR2 (0.3 ± 0.6 of 45.5 ± 13.4 Sst^+ neurons, $n = 3$ mice) or FLEX-Arch (2.0 ± 0.0 of 36.3 ± 9.8 Sst^+ neurons, $n = 3$) (**Fig. 1e**). EYFP and GFP expression colocalized with glycine immunoreactivity in both sets of mice (**Fig. 1f**).

[1]Department of Neurobiology, David Geffen School of Medicine, University of California, Los Angeles, California, USA. [2]Department of Physiology, West China School of Preclinical and Forensic Medicine, Sichuan University, Chengdu, Sichuan, People's Republic of China. Correspondence should be addressed to J.L.F. (feldman@ucla.edu).

Received 30 October 2014; accepted 7 January 2015; published online 2 February 2015; doi:10.1038/nn.3938

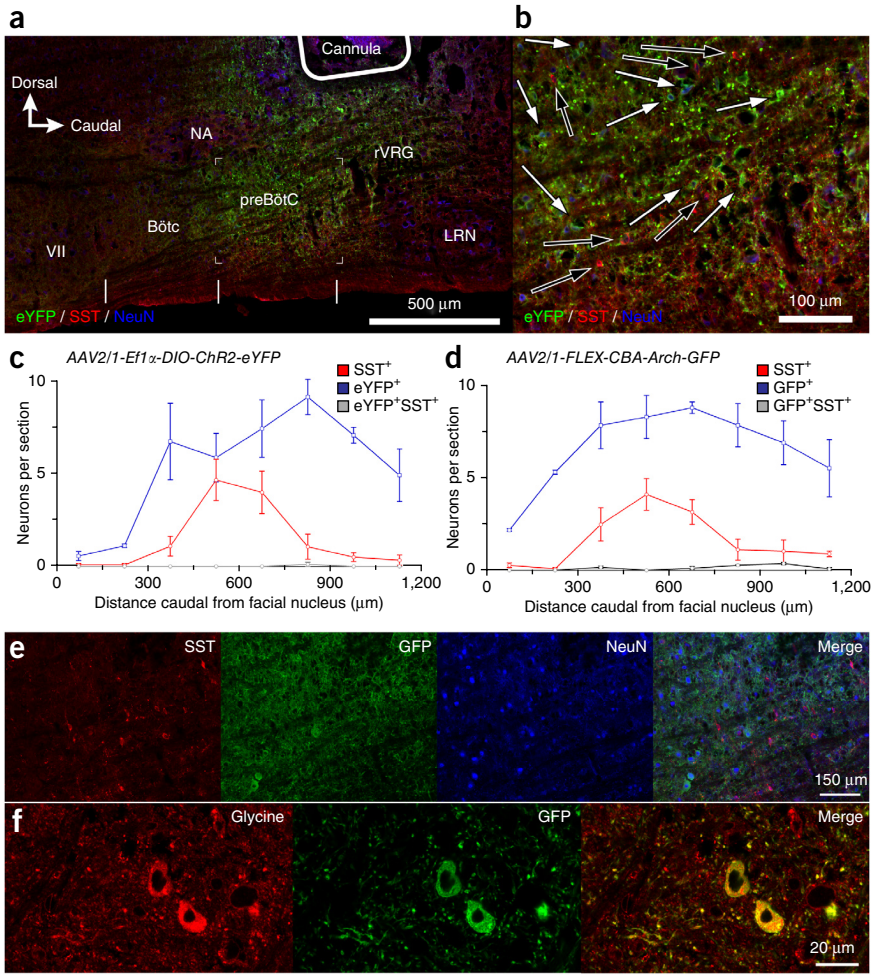

Figure 1 Cre-dependent ChR2 or Arch expression targeted to preBötC *Glyt2* neurons. (**a**) Representative confocal mosaic micrograph of sagittal brainstem section of *Glyt2-Cre* mouse showing the extent of eYFP$^+$ and Sst$^+$ neurons after injection of *AAV2/1-Ef1α-DIO-ChR2-eYFP* into preBötC (n = 5). Vertical white lines at bottom mark approximate rostral-caudal boundaries of BötC and preBötC. Top right, outline of cannula tip placement. No labeled somas were found in the brainstem outside the boundaries of this micrograph. VII, facial nucleus; NA, nucleus ambiguus; LRN, lateral reticular nucleus. (**b**) High-magnification micrograph of bracketed segment in **a** showing eYFP$^+$ preBötC neurons (white arrows) intermingled with Sst$^+$ neurons (black arrows). (**c**,**d**) Distribution of eYFP and GFP (blue line), marking location of neurons expressing ChR2 (**c**, n = 3) or Arch (**d**, n = 3) and *Sst*$^+$ (red line) neurons relative to caudal boundary of facial nucleus. Error bars represent mean ± s.e.m. (**e**) Representative single channel and overlay confocal micrographs showing eYFP$^+$ preBötC neurons (green) after *AAV2/1-Ef1α-DIO-ChR2-eYFP* injection. Section also labeled for Sst (red) and NeuN (blue) immunoreactivity. (**f**) Single channel and overlay confocal micrographs (n = 3) showing eYFP$^+$ preBötC neurons (green) with glycine immunoreactivity (red).

To efficiently deliver light specifically into the preBötC, we implanted optical cannulae bilaterally from a dorsal approach, about 200–400 µm dorsal to the preBötC (**Fig. 1a**,**b**). By placing the cannulae close to the preBötC, we ensured that the pool of light-responsive neuronal somas able to affect breathing were preBötC Glyt2 neurons. As delineated below, the most parsimonious explanation of our results is that the light-induced responses were a result of activation of preBötC Glyt2 neurons.

Brief photostimulation of ChR2-transfected preBötC Glyt2 neurons

In anesthetized Cre$^+$ mice, brief bilateral photostimulation (100-ms pulse, 473 nm; **Fig. 2a**) of ChR2-transfected preBötC Glyt2 neurons generated respiratory phase–dependent changes in breathing (n = 5). As revealed by phase response curves (Online Methods and **Fig. 2a**), ChR2 activation affected respiratory cycle timing, peak inspiratory airflow and inspiratory duration (**Fig. 2b–f**).

Bilateral photostimulation during early inspiration (ϕ_{stim} = 0–30°; **Fig. 2a**) resulted in premature inspiratory burst termination, that is, a breath with truncated peak inspiratory airflow (decreased to 56.4 ± 5.9% of control, $P = 10^{-10}$, n = 5; **Fig. 2c**,**e**) and shortened inspiratory duration (decreased to 67.5 ± 5.4% of control, $P = 10^{-10}$, n = 5; **Fig. 2c**,**f**). In contrast, stimulation during expiration (ϕ_{stim} = 180–360°) delayed the onset of the subsequent inspiration, with the strongest effect occurring during the late expiratory (ϕ_{stim} = 330–360°, often referred to as the pre-inspiratory (pre-I)) phase (**Fig. 2b**,**d**), with a 233 ± 20° shift ($P = 2 \times 10^{-10}$, n = 5), whereas stimulations falling earlier in expiration (ϕ_{stim} = 150–180°) produced a smaller 94 ± 16° shift (P = 0.007, n = 5; **Fig. 2b**). Following this phase shift, the next inspiration had no significant change in amplitude (101 ± 3% of control, P = 1, n = 5) or duration (104 ± 3% of control, P = 1, n = 5).

Prolonged photostimulation of ChR2-transfected preBötC Glyt2 neurons

In anesthetized ChR2-transfected mice, a 1-s photostimulus (7 × 100-ms pulses, 50-ms interpulse interval) at any time during the respiratory cycle stopped breathing, that is, produced an apnea, which continued until after the light shut off (n = 5; **Fig. 3a**). The subsequent respiratory cycle began at a fairly constant delay after the laser turned off regardless of stimulus phase (**Fig. 3b**,**c**). The duration of this delay was unique to each mouse (300–860 ms, min-max, n = 3), presumably as a result of differences in the precise position of the virus injection and optical fiber placement. When tested in awake mice, a 1-s pulse train consistently produced apneas (n = 5; **Fig. 3d**). We further tested photostimulus responses in anesthetized mice when ventilation was increased during 5 min of either hypoxic (8% O_2, 92% N_2, n = 5) or hypercapnic (5% CO_2 in room air, n = 5) inspired gas mixtures, finding that ChR2 activation still consistently produced apnea in either of these conditions of increased respiratory drive (**Fig. 3e**,**f**). Prolonged stimulation (up to 20-s pulse trains, n = 3) produced an apnea that persisted until the laser turned off (**Fig. 3g**).

Photoinhibition of Arch-transfected preBötC Glyt2 neurons

Pre-inspiratory or early inspiratory bilateral photoinhibition (ϕ_{stim} = −120 to 30°) of Arch-transfected preBötC *Glyt2* neurons (100-ms pulse, 593 nm, n = 7; **Fig. 4a**) increased peak inspiratory airflow (137.0 ± 3.8% of control, $P = 2 \times 10^{-9}$, n = 7) and tidal volume (**Fig. 4b**,**c**) without a significant change in inspiratory duration (103.0 ± 0.9% of control, P = 1, n = 7; **Fig. 4b**,**d**) or respiratory phase (P = 1, n = 7; **Fig. 4e**).

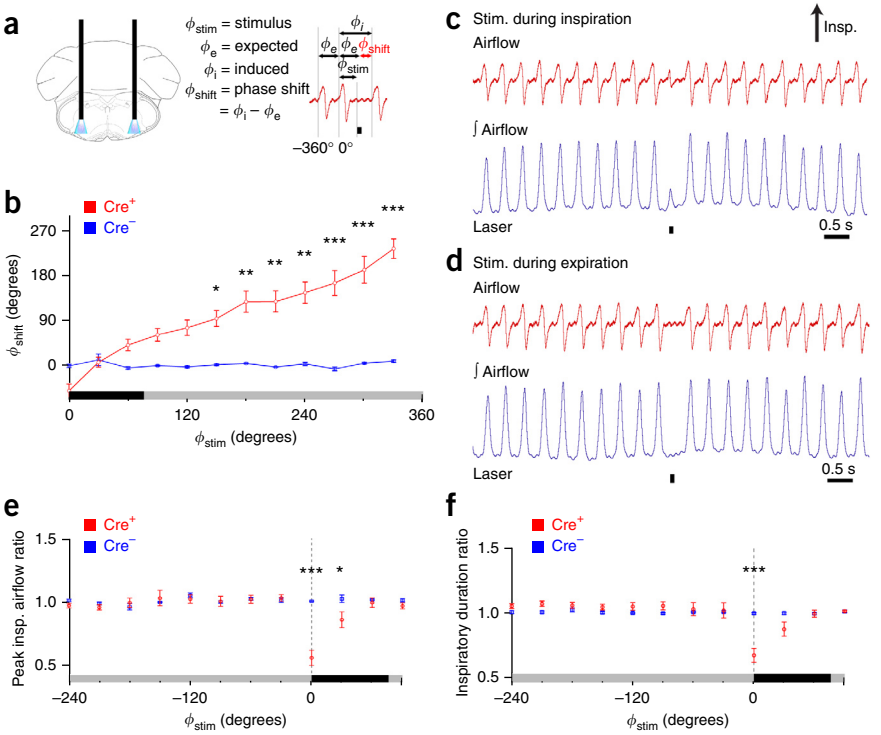

Figure 2 Photostimulation of preBötC Glyt2 neurons depresses breathing. (**a**) Left, schematic depicting bilateral placement of optical cannulae targeting preBötC. Right, schematic airflow trace depicting definitions of stimulus phase (ϕ_{stim}), expected phase (ϕ_e), induced phase (ϕ_i) and phase shift (ϕ_{shift}), demarcated with horizontal arrows, relative to the reference cycle that spans 0–360°; the control cycle preceding reference cycle spans phase –360–0°. Black bar below trace is laser-on period that defines the start of ϕ_{stim}. ϕ_e is the period of the previous control respiratory cycle, and ϕ_{shift} is the difference between ϕ_e and ϕ_i. (**b**) Shift in respiratory phase (ϕ_{shift}) resulting from bilateral photostimulation (100-ms pulse) of preBötC Glyt2 neurons in *Glyt2-Cre*$^+$ (Cre$^+$, red, $n = 5$) and *Glyt2-Cre*$^-$ (Cre$^-$, blue, $n = 5$) mice. Stimulus phase (ϕ_{stim}) is depicted on x axis (**b**,**e**,**f**) with inspiration (black bar) defined from 0–72°, with gray bar: (**b**) the subsequent expiration defined from 72–360° or (**e**,**f**) the preceding expiration defined from –288–0° (150–180°, $P = 0.007$; 180–210°, $P = 2 \times 10^{-5}$; 210–240°, $P = 4 \times 10^{-6}$; 240–270°, $P = 4 \times 10^{-7}$; 270–300°, $P = 1 \times 10^{-9}$; 300–330°, $P = 5 \times 10^{-10}$; 330–360°, $P = 4 \times 10^{-10}$). (**c**,**d**) Representative airflow and tidal volume (∫airflow) traces illustrating effect of photostimulation (100-ms pulse, black bar beneath trace) during inspiration (**c**) and expiration (**d**). (**e**,**f**) Comparison of ratio of peak inspiratory airflow (**e**; 0–30°, $P = 4 \times 10^{-10}$; 30–60°, $P = 0.02$) or inspiratory duration (**f**; 0–30°, $P = 4 \times 10^{-10}$) in *Glyt2-Cre*$^+$ (Cre$^+$, red) and *Glyt2-Cre*$^-$ (Cre$^-$, blue) anesthetized mice. Dotted vertical line (**e**,**f**) at 0° indicates onset of inspiration. Error bars represent mean ± s.e.m. Statistical significance was determined with a one-way ANOVA and pair-wise comparisons were made with Tukey's HSD test. $^*P < 0.05$, $^{**}P < 0.001$, $^{***}P < 10^{-8}$.

Compared with these photoinhibition-augmented breaths, sighs, that is, larger breaths endogenously generated periodically to hyperinflate the lungs, had greater amplitudes (**Fig. 4f**). Sighs had peak inspiratory airflows that were 173 ± 15% of control ($P = 10^{-5}$, $n = 7$) that was also statistically different from photoinhibition-induced augmented breaths ($P = 0.02$, $n = 7$). Bilateral photoinhibition during midexpiration (ϕ_{stim} = −210 to −120°) produced a shift in respiratory phase that manifested by an earlier onset of the subsequent inspiration (−52.3 ± 6.2° phase shift, $P = 8 \times 10^{-6}$, $n = 7$; **Fig. 4e**,**g**), with the strongest effect at −180 to −150°. Prolonged photoinhibition (5-s pulse) increased respiratory frequency, but the effect was transient and did not last for the full duration of the laser pulse ($n = 3$; **Fig. 4h**).

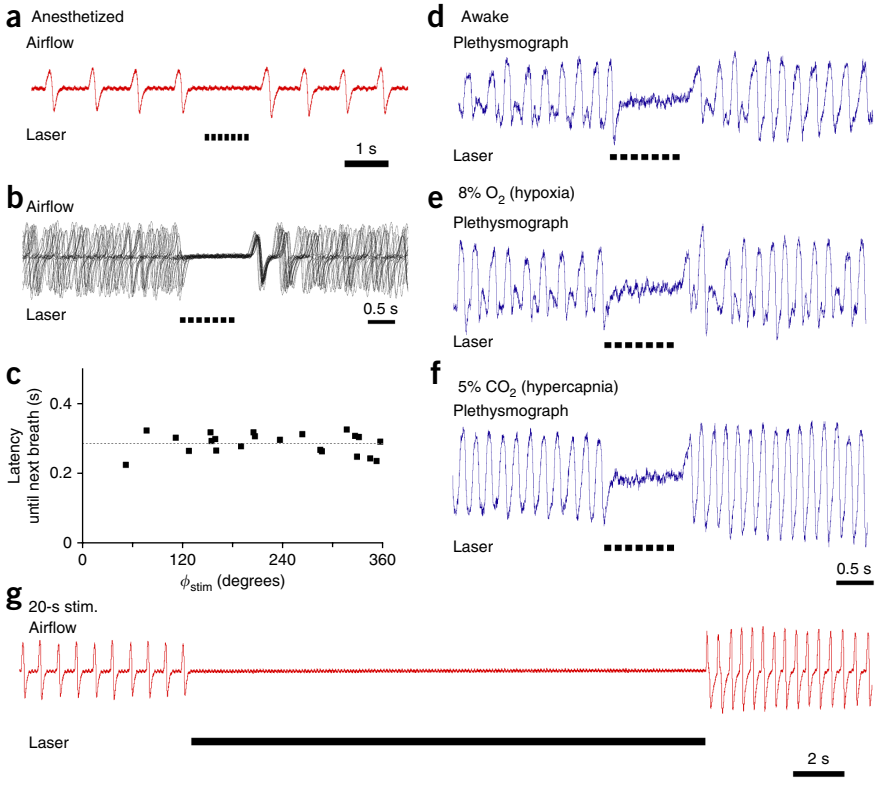

Figure 3 Prolonged photostimulation of preBötC Glyt2 neurons results in apnea. (**a**) Representative airflow trace illustrating effect of 1-s pulse train of photostimulation (black bars beneath trace, 7 × 100-ms pulses with a 50-ms interpulse interval, $n = 5$). (**b**) Overlay of airflow traces aligned to the laser onset at various phases of respiratory cycle (7 × 100-ms pulses with a 50-ms interpulse interval) reveals that the next breath occurred at a fairly constant delay after the laser shuts off. (**c**) Representative graph of latency to next breath as a function of initial phase of photostimulation. Dotted line indicates mean latency. (**d**–**f**) Photostimulation with a 1-s pulse train (7 × 100-ms pulses with 50-ms interpulse interval) of awake, behaving mice in a plethysmograph under eupneic (**d**; $n = 5$), hypoxic (**e**; $n = 5$) or hypercapnic (**f**; $n = 5$) states. (**g**) Airflow during bilateral 20-s pulse train of light (100-ms pulses with 50-ms interpulse interval, $n = 3$) in anesthetized mouse.

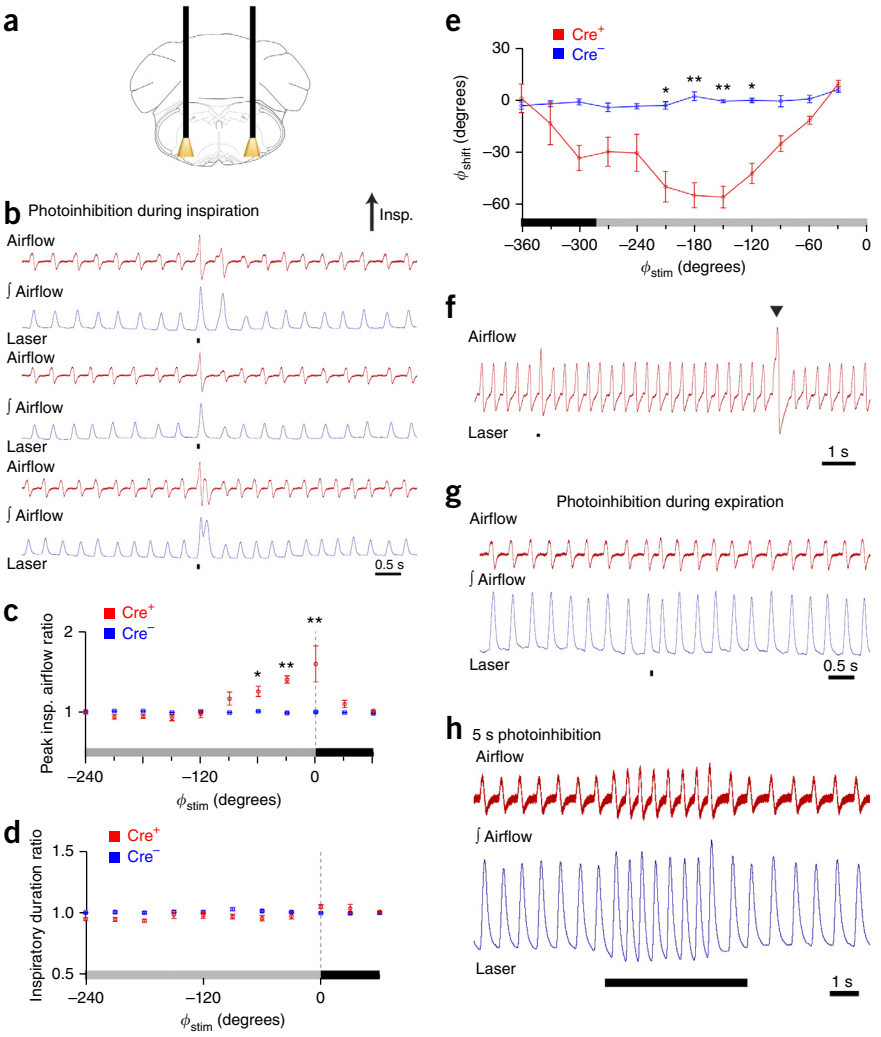

Figure 4 Photoinhibition of preBötC Glyt2 neurons augments breathing. (**a**) Schematic depicting bilateral placement of optical cannulae targeting preBötC. (**b**) Representative airflow and tidal volume (∫airflow) traces (three pairs) illustrating effect of brief photoinhibition (100-ms pulse, black bar) during inspiration. (**c**,**d**) Comparison of photoinhibited cycle to prior control cycle as a function of stimulus phase (ϕ_{stim}) for ratio of peak inspiratory airflow (**c**; $n = 7$; 0–30°, $P = 2 \times 10^{-7}$; 300–330°, $P = 0.01$; 330–360°, $P = 5 \times 10^{-7}$) or inspiratory duration (**d**; $n = 7$, all $P > 0.05$) in Cre$^+$ (red) and Cre$^-$ (blue) anesthetized mice. Respiratory stimulus phase (ϕ_{stim}) on *x* axis (**c**–**e**) with inspiration (black) defined from 0 to 78° (–360° to –282°) and expiration (gray) defined from 78–360° (–282° to 0°). The dashed vertical line (**c**,**d**) at 0° indicates onset of inspiration. (**e**) Shift in respiratory phase (ϕ_{shift}) resulting from preBötC-targeted laser pulses (100-ms pulse) in *Glyt2-Cre*$^+$ (Cre$^+$, red, $n = 7$) and *Glyt2-Cre*$^-$ (Cre$^-$, blue, $n = 5$) mice (150–180°, $P = 0.002$; 180–210°, $P = 2 \times 10^{-5}$; 210–240°, $P = 8 \times 10^{-6}$; 240–270°, $P = 0.01$). (**f**) Representative light response in response to photoinhibition (black bar) compared with endogenous sigh (arrow). (**g**) Representative airflow and tidal volume (∫airflow) traces illustrating effect of brief photoinhibition (100-ms pulse; black bar) during expiration. (**h**) Representative airflow and tidal volume traces illustrating that longer photostimulation (5-s continuous pulse) increased peak inspiratory airflow and frequency ($n = 3$). Error bars represent mean ± s.e.m. Statistical significance was determined with a one-way ANOVA and pair-wise comparisons were made with Tukey's HSD test. *$P < 0.05$, **$P < 0.001$.

Arch activation rescues breathing during a reflex apnea

A critical role of inhibition in the preBötC in controlling respiratory pattern is likely in the production of apneas[10], such as during swallowing or breathholding. To determine whether preBötC Glyt2 neurons participate in generating apneas, we photoinhibited these neurons during Breuer-Hering lung inflation reflex (BHIR)-induced apneas[10]. The lungs were inflated with sufficient continuous positive airway pressure (CPAP) to produce apneas that lasted ~11 s (~4-cm H_2O) during control periods (**Fig. 5a**). Photoinhibiting Arch-transfected preBötC Glyt2 neurons (1 s pulse) broke the apnea with one or two breaths ($n = 3$; **Fig. 5a**). Laser onset at 5.5 ± 0.5 s after onset of CPAP (CPAP + laser) induced a first breath at 5.8 ± 0.5 s, that is, a 300-ms delay from the laser onset versus an expected first breath at 11.8 ± 1.4 s during control (CPAP only) periods (ANOVA, $P = 3 \times 10^{-6}$, $n = 3$; **Fig. 5b**).

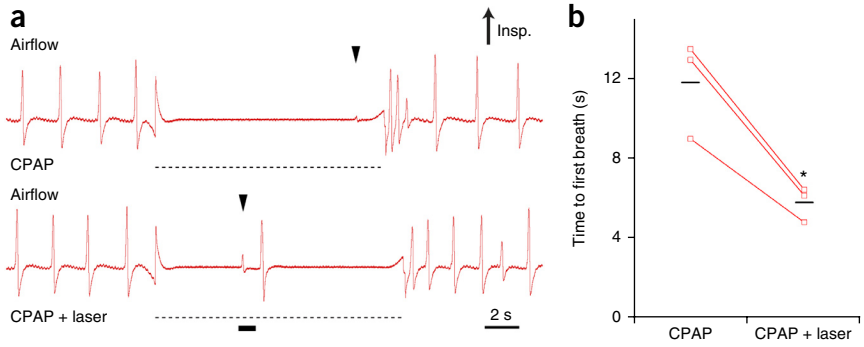

Figure 5 Photoinhibition of preBötC Glyt2 neurons during a reflex apnea rescues breathing. (**a**) BHIR triggered by continuous positive airway pressure (CPAP, ~4-cm H_2O, dashed black line) induced apnea in a tracheotomized, anesthetized Arch-transfected mouse in control (top) and bilateral photoinhibition (bottom, black bar) conditions. Top, after onset of BHIR, first breath was at ~11 s (black arrow). Bottom, 1-s pulse applied 5.5 ± 0.5 s from onset of BHIR produced a first breath (indicated with a black arrow) 5.8 ± 0.5 s after the start of reflex, that is, a 300-ms delay from the laser onset, versus an expected first breath at 11.8 ± 1.4 s, as seen during control (CPAP only) periods. (**b**) Duration of induced apnea, measured from onset of BHIR to onset of the next inspiration, in CPAP only and CPAP + laser conditions. Means are indicated with black horizontal lines ($n = 3$, $P = 3 \times 10^{-6}$). Statistical significance was determined with an unpaired *t* test. *$P < 10^{-5}$.

Single-unit recording in ChR2- and Arch-transfected mice

In ChR2-transfected mice, we unilaterally photostimulated (1-s pulse) and recorded from preBötC neurons in the cone of light (n = 18 in 3 mice; **Fig. 6a**). Unilateral ChR2 photostimulation of preBötC Glyt2 neurons was sufficiently strong to recreate the effects observed from bilateral photostimulation, that is, a persistent apnea during the photostimulation period (for example, **Fig. 2g**). In total, we recorded 18 neurons, of which eight were respiratory modulated (five neurons were pre-I, two were inspiratory and one was expiratory; **Fig. 6b**) and ten neurons fired tonically. All of the recorded respiratory-modulated neurons and all but two of the tonically firing neurons were silenced during photostimulation. The onset of the next inspiration following photostimulation was delayed relative to the expected phase (**Fig. 6b**). Pre-I neurons could be silenced at any point in the respiratory cycle. When silenced early enough in the pre-I phase, the initial preBötC activity was not followed by burst firing, motor output or the onset of inspiratory airflow (**Fig. 6b**). The delay between the laser shutting off and the onset of the next breath (described above; **Fig. 3b**) was also seen in the preBötC neuron firing pattern. While recording in the preBötC, we consistently observed a short-lasting multi-unit field potential after laser onset, consistent with (transient) activation of neighboring Glyt2 neurons (**Fig. 6c**).

In Arch-transfected mice, we recorded from preBötC neurons during unilateral photoinhibition (1-s pulse, n = 12 units in 2 mice), finding seven respiratory-modulated neurons (two pre-I neurons, two inspiratory neurons, one post-inspiratory (or early-expiratory) neuron and one expiratory neuron; **Fig. 6d**) and five tonic neurons. Unilateral photoinhibition generated shifts in the respiratory cycle, comparable to that observed during bilateral photoinhibition, but did not alter peak inspiratory airflow. During photoinhibition, preBötC neurons exhibited a shorter interval between inspirations, consistent with changes in the breathing pattern (**Fig. 6d**). We did not find any neurons that increased their firing during delivery of light pulses, which may be reflective of unilateral photoinhibition not altering inspiratory amplitude. We also found two tonic neurons that were silenced in response to light from a baseline firing rate of ~16 Hz (for example, see **Fig. 6d**). Following a 1-s light pulse, these neurons exhibited rebound firing after the laser shut off. The remaining neurons did not change their firing pattern or phase relationship to breathing during photoinhibition.

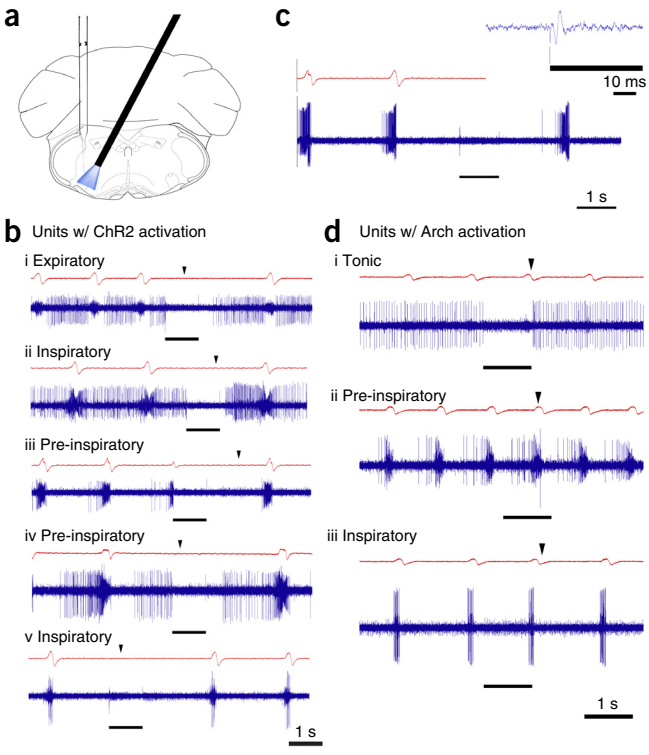

Figure 6 Unit recording with concurrent ChR2 or Arch activation. (**a**) Schematic showing cannulae implantation at a 27° angle and vertical electrode placement to record from units within the cone of light (473 nm or 593 nm) in opsin-transfected mice. (**b**) Representative airflow traces (red) and respiratory-modulated units (blue; i, expiratory; ii, inspiratory; iii, pre-inspiratory; iv, pre-inspiratory; v, inspiratory) showing strong inhibition during 1-s continuous laser pulse (black bar). Black arrows indicate the expected onset of inspiration following photostimulation. In total, 18 neurons were recorded from 3 mice. (**c**) Representative recording of multiple units following photostimulation of ChR2-expressing preBötC Glyt2 neurons with airflow trace. Inset, shorter timescale at onset of continuous laser pulse (black line) showing large field potential within ~2 ms. Vertical black line shows alignment of laser onset and initial artifact on trace. (**d**) Response of preBötC neurons (blue; i, tonic; ii, pre-inspiratory; iii, inspiratory) to photoinhibition of Arch-expressing preBötC Glyt2 neurons with 1-s continuous laser pulse (black line). Black arrows indicate the expected onset of inspiration following photoinhibition as measured on the airflow trace. In total, 12 neurons were recorded from 2 mice.

DISCUSSION

Inhibition is an essential element of most neural circuits in the mammalian nervous system. Although Glyt2$^+$ inhibitory neurons are present in the preBötC and in slices *in vitro*, ~20% of these neurons are inspiratory modulated and ~50% are tonic (we do not know what percentage are respiratory modulated, tonic or silent *in vivo*, and under which physiological conditions)[3,11], their functional role in the generation of respiratory rhythm and pattern is not well understood and is disputed[10,17]. Strong inhibitory currents are observed in intracellular recordings of preBötC neurons in deeply anesthetized rats and cats[8]. Although a normal rhythmic breathing pattern remains in the absence of conventional postsynaptic inhibition in the preBötC[10,18], inhibitory modulation is important for preBötC dynamics[8]. By making temporally precise brief bilateral perturbations of preBötC Glyt2 neurons, we probed their role in the generation of respiratory pattern in spontaneously breathing adult mice.

We used conditional gene targeting for restricting protein expression to inhibitory preBötC neurons. Given that the *Glyt2* promoter is specific to glycinergic neurons[15], by locally injecting Cre recombinase–dependent viruses into the preBötC of transgenic mice expressing Cre driven by the *Glyt2* promoter[12–14], we were able to selectively activate and silence these inhibitory neurons specifically in the preBötC of intact, awake or anesthetized, spontaneously breathing mice. To verify this, we examined the overlap of transfected neurons with known markers of excitatory or inhibitory neurons. We found that transfected neurons rarely colocalized with *Sst*, which demarcates a subset of excitatory preBötC neurons, and colocalized with glycine immunoreactivity, which identifies glycinergic neurons.

Our injection sites were centered on the preBötC, with some Glyt2$^+$ neuronal somas transfected rostrally including in the BötC, which also contains substantial numbers of respiratory-modulated inhibitory, including glycinergic, neurons[19–21], caudally in the rostral ventral respiratory group that contains bulbospinal inspiratory neurons projecting to phrenic and intercostal motoneurons, and dorsally in the adjacent reticular formation. Peak densities of transfected neurons substantially overlapped with the distribution of *Sst*$^+$ neurons relative to the caudal boundary of the facial nucleus, indicating

that we successfully hit the preBötC. Optical cannulae were placed 200–400 µm dorsal to the caudal end of the preBötC to limit the light path to mainly target the somas of preBötC neurons and avoid the somas of transfected neurons outside the preBötC. However, opsins are not localized to any one neuronal domain (including expression in synaptic terminals), so there is the possibility that light affected synaptic terminals in the preBötC that originated from transfected somas adjacent to its boundaries. Insofar as these axons and presynaptic terminals arose from somas in the preBötC (including from the contralateral side), the results reflect the effects of perturbing preBötC Glyt2 neuron excitability. Of concern are effects that may have resulted from stimulating axons and presynaptic terminals of Glyt2 neurons with somas outside, but synapsing in, the preBötC. At the rostrocaudal level of the preBötC, neurons adjacent to the VRC do not have any respiratory-modulated activity[22] and have no established monosynaptic projections to the preBötC[23,24]. Thus, we consider the likelihood that glycinergic neurons at this level outside of the preBötC could have contributed to the observed responses to be small. Caudal to the preBötC in the VRC there are inspiratory neurons, mostly bulbospinal, with no known monosynaptic rostral projections to the preBötC[23,24]. Rostral to the preBötC in the VRC is the BötC, which contains a considerable number of Glyt2$^+$ neurons that appear to project to the preBötC; if photoactivation (ChR2) or photoinhibition (Arch) affected their terminals, then they could contribute to responses evoked when light was confined to the preBötC. By aiming at the caudal preBötC with our injection and cannulae placement, we avoided most, but not all, BötC neuronal somas, but may have affected some of their putative transfected terminals in the preBötC. If BötC and preBötC Glyt2 neurons constitute a functionally homogeneous population (which is presently unknown), then we have no concern. If they represent two distinct populations with different effects, then our interpretation of the source of the observed effects, that is, preBötC and/or BötC, would need to be parceled out. The most parsimonious explanation for our results is that light-activated responses are predominately from perturbations affecting preBötC Glyt2 neurons, including their terminals, and we frame the subsequent discussion accordingly.

Brief photoinhibition of Arch-expressing preBötC Glyt2 neurons during the pre-I or inspiratory phases produced significantly larger inspirations with no change in inspiratory duration. Thus, at least a subset of transfected Glyt2 neurons was endogenously active during (pre)inspiration and affected the amplitude of inspiratory outflow without an obligatory effect on its termination. If these neurons were essential for rhythmogenesis, one would predict that their photoinhibition during inspiration would also lengthen inspiratory duration. This was not the case when silencing a subset of these neurons sufficient to substantially increase inspiratory amplitude (**Fig. 4b–d**). We suggest that these data further support previous observations that rhythmogenesis *per se* is not particularly sensitive to changes in inhibition[10]. When photoinhibition occurred during mid-expiration, expiratory duration was shortened. Thus, withdrawal of inhibition during mid-expiration allows preBötC pre-I activity to initiate earlier and/or spread through the network more rapidly[25], resulting in inspiration being triggered sooner than expected. These data are consistent with the interpretation that these neurons can modulate respiratory timing.

Brief photostimulation of ChR2-expressing preBötC *Glyt2* neurons when delivered during the inspiratory phase prematurely terminated inspiration, that is, shorter inspiratory durations and smaller peak inspiratory airflows. Photostimulation during expiration, including the pre-I phase, lengthened that phase, significantly delaying the subsequent inspiration. In response to longer stimuli, this effect was sufficiently strong to produce apnea in anesthetized or awake mice at rest, as well as when ventilation was increased by hypoxic or hypercapnic challenges. We found that respiration resumed with a consistent latency after the laser shut off regardless of the phase of photostimulation, which indicates that activation of preBötC Glyt2 neurons can reset the respiratory cycle.

Activation of preBötC *Glyt2* neurons inhibits other respiratory-modulated preBötC neurons. We found 7 (pre)inspiratory-modulated neurons in total and all were silenced by ChR2 activation, at any point in the respiratory cycle. Silencing pre-I neurons before the start of inspiration coincided with typical pre-I spiking activity that was not followed by an inspiratory burst. That initial pre-I activity can occur without a subsequent burst is consistent with our hypothesis that inspiratory burst initiation and patterning are separate components of a two-stage process that can be experimentally decoupled[25]. We conclude that preBötC *Glyt2* neurons can modulate the activity of rhythmogenic preBötC neurons and, when activated, can prematurely terminate an inspiratory burst, but that rhythmogenesis is not particularly sensitive to changes in inhibition.

We suggest that one essential role of preBötC *Glyt2* inhibitory neurons is to modulate basic breathing parameters such as inspiratory flow, tidal volume, inspiratory and expiratory duration, and respiratory frequency, irrespective of any role in rhythmogenesis *per se*. By modulating the activity of preBötC *Glyt2* neurons, we were able to, in effect, tune the dynamics of the preBötC network.

We did not isolate any neurons that were activated by photostimulation. There are several possibilities. First, our sample size was too small. Second, photostimulation activated a substantial number of preBötC Glyt2 neurons that were silent under control conditions and were therefore not isolated before stimulation. At present, we do not know the fraction of preBötC Glyt2 neurons that are respiratory modulated or tonically active in anesthetized spontaneously breathing mice, and we have to allow for the possibility that this fraction is small. Third, laser light caused rapid, potent and, as long as the light was on, continual release of glycine from synaptic terminals of the transfected neurons. This would rapidly terminate the activity of all preBötC, including glycinergic, neurons. Thus, glycine could continue to be released during the entire duration of stimulation while all neurons were silent. The multi-unit field potential observed after laser onset may be the signature of transient activation of nearby Glyt2 neurons (**Fig. 6c**).

Numerous models of central pattern generation focus on inhibition as a key component in the generation of rhythmic behaviors[26–29]; for breathing, inspiratory burst termination and/or phase transitions are often postulated to be mediated by postsynaptic actions of inhibitory neurons[9,30,31]. One recent model postulates that interactions between excitatory preBötC neurons and inhibitory subpopulations in the preBötC and BötC are essential for generating a normal respiratory rhythm[17]. However, although marked changes in breathing result from slow or relatively rapid onset perturbations to excitatory preBötC subpopulations[1,5], a normal respiratory rhythm persists in anesthetized adult rats after substantial blockade of inhibitory neurotransmission in preBötC and BötC by local injection of $GABA_A$ and glycine antagonists[10]. Our data are consistent with this result. We did not observe any breakdown in eupneic breathing when silencing a subset of preBötC Glyt2 neurons that was nonetheless sufficient to substantially increase inspiratory amplitude (**Fig. 4b–d**). Whether silencing a larger percentage of the preBötC Glyt2 neurons affects rhythmogenesis *per se* remains to be determined. Thus, we consider it unlikely that preBötC inhibitory neurons have an obligatory role in terminating inspiration.

Photoinhibition of preBötC Glyt2 neurons increased respiratory drive, producing larger breaths at a higher frequency. Thus, the preBötC

in vivo with diminished preBötC Glyt2 neuronal activity, but otherwise intact, continued to generate a eupneic breathing rhythm[10]. Photoinhibition did not change the firing of pre-I neurons, suggestive of weak or absent Arch expression in these neurons. We do not know from our experiments whether these neurons were excitatory, that is non-Glyt2, or simply failed to express sufficient protein. As we did not observe increased activity in pre-I neurons, we suggest that either unilateral photoinhibition of preBötC *Glyt2* is not sufficient to induce changes in individual pre-I neurons or the increased respiratory drive results from an increase in the total number of active neurons, and not the number of spikes *per se*.

Precisely timed apneas are an essential component of many vital, complex oropharyngeal movements, for example, swallowing, vocalization, suckling and chewing, and there are many powerful reflex apneas, such as the BHIR or following superior laryngeal nerve activation[32–34] that can be triggered by tracheal obstruction. We hypothesize that inhibitory neurons are important for the generation of central apneas[10]. In support of this hypothesis and refining the experimental protocol to target the preBötC, we found that prolonged photostimulation of preBötC Glyt2 neurons initiated at any point in the respiratory cycle could produce apnea. Moreover, photoinhibition of preBötC *Glyt2* neurons were able to counteract a reflex-induced apnea generated by the BHIR (**Fig. 5a**).

In summary, we employed a virus-based strategy to selectively introduce ChR2 or Arch into inhibitory preBötC neurons. By delivering light into the preBötC via chronically implanted optical cannulae in transfected anesthetized or awake mice, we found that preBötC Glyt2 neuronal activity modulates the respiratory output, and may be critical in the manifestation and control of apneas essential for normal behavior, but does not appear to be an essential component underlying respiratory rhythmogenesis. Finally, the phase-response curves for photostimulation and photoinhibition represent a new class of data whose reproduction represents an essential test for any model purporting to explain respiratory rhythmogenesis.

METHODS

Methods and any associated references are available in the online version of the paper.

Note: Any Supplementary Information and Source Data files are available in the online version of the paper.

ACKNOWLEDGMENTS

The authors thank G. Li for excellent technical work and N. Brecha, T. Otis and K. Kam for thoughtful discussion. This work was supported by US National Institutes of Health grants NS72211 and NS58280.

AUTHOR CONTRIBUTIONS

D.S. and J.L.F. conceived of the study and designed the experiments. D.S. performed the experiments with help from J.W.W. and Y.C., and D.S. and J.W.W. analyzed the data. D.S. and J.L.F. made the figures and wrote the manuscript with help from J.W.W.

COMPETING FINANCIAL INTERESTS

The authors declare no competing financial interests.

1. Tan, W. *et al.* Silencing preBotzinger complex somatostatin-expressing neurons induces persistent apnea in awake rat. *Nat. Neurosci.* **11**, 538–540 (2008).
2. Smith, J.C., Ellenberger, H.H., Ballanyi, K., Richter, D.W. & Feldman, J.L. Pre-Botzinger complex: a brainstem region that may generate respiratory rhythm in mammals. *Science* **254**, 726–729 (1991).
3. Winter, S.M. *et al.* Glycinergic interneurons are functionally integrated into the inspiratory network of mouse medullary slices. *Pflugers Arch.* **458**, 459–469 (2009).
4. Stornetta, R.L. *et al.* A group of glutamatergic interneurons expressing high levels of both neurokinin-1 receptors and somatostatin identifies the region of the pre-Botzinger complex. *J. Comp. Neurol.* **455**, 499–512 (2003).
5. Bouvier, J. *et al.* Hindbrain interneurons and axon guidance signaling critical for breathing. *Nat. Neurosci.* **13**, 1066–1074 (2010).
6. Gray, P.A. *et al.* Developmental origin of preBotzinger complex respiratory neurons. *J. Neurosci.* **30**, 14883–14895 (2010).
7. Koizumi, H. *et al.* Structural-functional properties of identified excitatory and inhibitory interneurons within pre-Botzinger complex respiratory microcircuits. *J. Neurosci.* **33**, 2994–3009 (2013).
8. Richter, D.W. & Smith, J.C. Respiratory rhythm generation *in vivo*. *Physiology (Bethesda)* **29**, 58–71 (2014).
9. Ballantyne, D. & Richter, D.W. Post-synaptic inhibition of bulbar inspiratory neurones in the cat. *J. Physiol. (Lond.)* **348**, 67–87 (1984).
10. Janczewski, W.A., Tashima, A., Hsu, P., Cui, Y. & Feldman, J.L. Role of inhibition in respiratory pattern generation. *J. Neurosci.* **33**, 5454–5465 (2013).
11. Morgado-Valle, C., Baca, S.M. & Feldman, J.L. Glycinergic pacemaker neurons in preBotzinger complex of neonatal mouse. *J. Neurosci.* **30**, 3634–3639 (2010).
12. Deisseroth, K. *et al.* Next-generation optical technologies for illuminating genetically targeted brain circuits. *J. Neurosci.* **26**, 10380–10386 (2006).
13. Chow, B.Y. *et al.* High-performance genetically targetable optical neural silencing by light-driven proton pumps. *Nature* **463**, 98–102 (2010).
14. Lin, J.Y., Lin, M.Z., Steinbach, P. & Tsien, R.Y. Characterization of engineered channelrhodopsin variants with improved properties and kinetics. *Biophys. J.* **96**, 1803–1814 (2009).
15. Chalphin, A.V. & Saha, M.S. The specification of glycinergic neurons and the role of glycinergic transmission in development. *Front. Mol. Neurosci.* **3**, 11 (2010).
16. Cardin, J.A. *et al.* Driving fast-spiking cells induces gamma rhythm and controls sensory responses. *Nature* **459**, 663–667 (2009).
17. Smith, J.C., Abdala, A.P., Koizumi, H., Rybak, I.A. & Paton, J.F. Spatial and functional architecture of the mammalian brain stem respiratory network: a hierarchy of three oscillatory mechanisms. *J. Neurophysiol.* **98**, 3370–3387 (2007).
18. Shao, X.M. & Feldman, J.L. Respiratory rhythm generation and synaptic inhibition of expiratory neurons in pre-Botzinger complex: differential roles of glycinergic and GABAergic neural transmission. *J. Neurophysiol.* **77**, 1853–1860 (1997).
19. Schreihofer, A.M., Stornetta, R.L. & Guyenet, P.G. Evidence for glycinergic respiratory neurons: Botzinger neurons express mRNA for glycinergic transporter 2. *J. Comp. Neurol.* **407**, 583–597 (1999).
20. Jiang, C. & Lipski, J. Extensive monosynaptic inhibition of ventral respiratory group neurons by augmenting neurons in the Botzinger complex in the cat. *Exp. Brain Res.* **81**, 639–648 (1990).
21. Ezure, K., Tanaka, I. & Kondo, M. Glycine is used as a transmitter by decrementing expiratory neurons of the ventrolateral medulla in the rat. *J. Neurosci.* **23**, 8941–8948 (2003).
22. Alheid, G.F. & McCrimmon, D.R. The chemical neuroanatomy of breathing. *Respir. Physiol. Neurobiol.* **164**, 3–11 (2008).
23. Dobbins, E.G. & Feldman, J.L. Brainstem network controlling descending drive to phrenic motoneurons in rat. *J. Comp. Neurol.* **347**, 64–86 (1994).
24. Dobbins, E.G. & Feldman, J.L. Differential innervation of protruder and retractor muscles of the tongue in rat. *J. Comp. Neurol.* **357**, 376–394 (1995).
25. Kam, K., Worrell, J.W., Ventalon, C., Emiliani, V. & Feldman, J.L. Emergence of population bursts from simultaneous activation of small subsets of preBötzinger complex inspiratory neurons. *J. Neurosci.* **33**, 3332–3338 (2013).
26. Burns, B.D. The central control of respiratory movements. *Br. Med. Bull.* **19**, 7–9 (1963).
27. Bradley, G.W., von Euler, C., Marttila, I. & Roos, B. A model of the central and reflex inhibition of inspiration in the cat. *Biol. Cybern.* **19**, 105–116 (1975).
28. von Euler, C. On the central pattern generator for the basic breathing rhythmicity. *J. Appl. Physiol.* **55**, 1647–1659 (1983).
29. Feldman, J.L. & Cowan, J.D. Large-scale activity in neural nets II: a model for the brainstem respiratory oscillator. *Biol. Cybern.* **17**, 39–51 (1975).
30. Richter, D.W. Generation and maintenance of the respiratory rhythm. *J. Exp. Biol.* **100**, 93–107 (1982).
31. Schmid, K., Foutz, A.S. & Denavit-Saubie, M. Inhibitions mediated by glycine and GABAA receptors shape the discharge pattern of bulbar respiratory neurons. *Brain Res.* **710**, 150–160 (1996).
32. Xia, L., Damon, T., Niblock, M.M., Bartlett, D. & Leiter, J.C. Unilateral microdialysis of gabazine in the dorsal medulla reverses thermal prolongation of the laryngeal chemoreflex in decerebrate piglets. *J. Appl. Physiol.* **103**, 1864–1872 (2007).
33. Curran, A.K., Xia, L., Leiter, J.C. & Bartlett, D. Jr. Elevated body temperature enhances the laryngeal chemoreflex in decerebrate piglets. *J. Appl. Physiol.* **98**, 780–786 (2005).
34. Heman-Ackah, Y.D., Pernell, K.J. & Goding, G.S. The laryngeal chemoreflex: an evaluation of the normoxic response. *Laryngoscope* **119**, 370–379 (2009).

ONLINE METHODS

Animals. Animal use was in accordance with the guidelines approved by the University of California at Los Angeles Institutional Animal Care and Use Committee. Animals were housed in a vivarium under a 12-h light cycle with free access to food and water. All experiments were done on adult male *Glyt2-Cre* mice (24–30 g, C57Bl6 background, average post-surgery duration of ~30 d) with peripheral nerves, for example, vagus, carotid sinus nerve intact, that were 10–14 weeks of age at the time of AAV injection. Prior to surgery, animals were housed in groups of variable size up to five mice per cage; after surgery, animals were housed individually as required by our study protocols. Mice breathed spontaneously. The *Glyt2-Cre* mice were kindly provided by H.U. Zeilhofer (University of Zurich).

Viral vector design. The viral constructs *AAV2/1-Ef1α-DIO-ChR2-eYFP* (Addgene plasmid 20298; provided by K. Deisseroth, Stanford University)[16] and *AAV2/1-flex-CBA-Arch-GFP* (Penn Vector P2432; provided by E. Boyden, Massachusetts Institute of Technology)[13] were produced by the University of Pennsylvania Gene Therapy Program Vector Core. We used a ChR2 variant with the H134R mutation, which produces a twofold increase in the steady-state current as compared to the wild-type variant of ChR2 (refs. 35,36).

Microinjection. Mice were anesthetized with isoflurane (4% for induction and 2% for maintenance, wt/vol) and placed in a stereotaxic apparatus (David Kopf Instruments) with Bregma and Lambda skull landmarks level. Two holes were drilled in the skull at predefined coordinates relative to Bregma to allow the insertion of glass pipettes containing a virus solution (ChR2, $5–10 \times 10^{12}$ genome copies per ml; Arch, $6–10 \times 10^{12}$ genome copies per ml) connected to a pressure ejection system (Picospritzer II, Parker Hannafin) targeted to the preBötC. Once situated, 100–200 nl per side was injected into the preBötC. Injections were made 6.80 mm caudal to Bregma, 1.20 mm lateral to the midline, and 4.65 mm ventral from the dorsal surface of the brain. Coordinates were determined from microinjections ($n = 7$) of red fluorescent microspheres (1.0 µm diameter, 5% solution, Invitrogen) into calculated coordinates based on a mouse brain atlas[37] and adjusted based on the distance from preBötC, as determined by the location of *Sst*-immunoreactive neurons[4]. The pipette was left in place for 5 min after injection to minimize backflow. The wound was closed with 5–0 non-absorbable sutures. The mice were returned to their home cage and allowed 2–3 weeks to recover, allowing time for sufficient levels of protein to express. For controls, negative littermates (those not expressing Cre recombinase) received virus injections as described above; as expected, there was no virus expression. Microinjections of Cre-dependent virus were performed with the investigator blind to whether the animal was Cre^+ or Cre^-.

Implantation of fiber optics. Mice were placed into the stereotaxic frame and fiber-optic cannulae with a 1.25-mm stainless steel ferrule (200 µm fiber; Doric Lenses), held by a stereotaxic adaptor (Doric Lenses), were implanted bilaterally to a depth 200–400 µm dorsal to the preBötC, based on predetermined coordinates. The cannulae were glued to the skull using Metabond (Parkell) and the wound was sealed by applying a layer of clear dental acrylic (Lang Dental).

Photostimulation and photoinhibition. Branching optical fibers (200-µm fiber, Doric Lenses) with 1.25-mm stainless steel ferrules as ends were connected to the implanted cannulae via plastic sleeves. The back end of the fiber was connected to a 473-nm/593-nm dual wavelength laser (OptoDuet Laser, IkeCool) via an optical rotary joint (Doric Lenses). Light pulses were controlled by a pulse generator (Pulsemaster A300 Generator; WPI). Anesthetized mice were placed on a heating pad and in front of a nose cone connected to a flowmeter (GM Instruments) to record airflow. Awake mice were placed in a plethysmograph chamber (Buxco) connected to a pressure transducer (F.W. Kirk Company) with the optical fibers exiting the chamber through a small hole.

BHIR. The BHIR was induced in anesthetized Arch transfected mice (FLEX-Arch) by inflating the lungs with continuous positive airway pressure (CPAP). The pressure was adjusted to yield an apnea that lasted for ~10 – 15 s (~4 cm of H_2O) before being 'broken' by breaths reappearing despite the CPAP. We applied one control period of CPAP, waited for 30–60 s, and then applied a second period of CPAP combined with a 1-s pulse of light (593 nm) delivered bilaterally into the preBötC. We measured both the amount of time it took for breathing to resume relative to the start of the reflex and the onset of the laser pulse.

Single-unit recording. To record neuronal activity, transfected mice were placed in the stereotaxic frame as described above. An optical cannula was implanted at a 27° angle from vertical, tilted across the midline from right to left, down to preBötC and glued to the skull with Metabond (Parkell). A window was drilled through the skull of sufficient size to allow the recording electrode free range of movement to record on the left side of the brain. Respiratory-modulated units were found 4.6 to 4.9 mm below the cerebellar surface and 1.1 to 1.3 mm lateral to the midline. A glass electrode (~3-µm inner tip diameter; filled with artificial cerebrospinal fluid containing (in mM) 124 NaCl, 3 KCl, 1.5 $CaCl_2$, 1 $MgSO_4$, 25 $NaHCO_3$, 0.5 NaH_2PO_4, and 30 D-glucose) was connected to a headstage (Siskiyou) and the signal amplified (Grass Model P511, Grass Instruments) and sampled at 20 kHz (PowerLab 16SP, ADInstruments). Due to a laser artifact apparent at the start and end of laser pulses, we used a single 1-s pulse for photostimulation to reduce noise. Most neural recordings were stable for 5–10 min.

Histology. After the completion of the experiment, mice were deeply anesthetized with pentobarbital and perfused transcardially with saline followed by 4% paraformaldehyde (wt/vol) in phosphate-buffered saline (PBS). Brains were removed, postfixed overnight at 4 °C, and cryoprotected in 30% sucrose (wt/vol) in PBS for 24–48 h before sectioning. Free-floating coronal or sagittal sections (40 µm) were cut using a cryostat (CryoStar NX70, Leica Microsystems) in two series and stored at 4 °C until further processing. Sections were incubated with primary antibodies in PBS containing 0.3% Triton X-100 ((vol/vol) PBT) overnight at 20–25 °C. After three washes, sections were incubated in species-appropriate secondary antibodies in PBS for 4 h at 20–25 °C. After three washes, sections were mounted onto gelatin-coated glass slides, dehydrated in graded alcohols, cleared in Xylenes and coverslipped. Fluorescence was visualized with a confocal laser-scanning microscope (LSM710, Carl Zeiss). Images were acquired with Zen software (Carl Zeiss), exported as TIFF files, and arranged to prepare figures in Photoshop and Illustrator (Adobe).

We used the following primary antibodies: rabbit polyclonal antibody to somatostatin-14 (1:500; Peninsula Laboratories; T4103), mouse monoclonal antibody to NeuN (1:500; Millipore; MAB377), chicken polyclonal antibody to GFP (1:500; Aves Labs; GFP-1020) and rabbit antibody to glycine (1:500; Millipore; AB5020). Rhodamine Red-X donkey antibody to rabbit, DyLight488 or Cy2 donkey antibody to chicken, and Cy5 donkey antibody to mouse conjugated secondary antibodies (1:250; Jackson ImmunoResearch) were used to detect primary antibodies. These four antibodies are frequently used in mice and have been well validated. The validity of the SST-14 antibody has been shown in both rat[1,38] and mice[5,25]. The GFP antibody has used successfully in mice as well[5]. In addition, the glycine antibody has been extensively used and validated as a marker of glycinergic neurons in mice and rats[39,40]. The NeuN antibody has been extensively used in mice throughout the field of neuroscience research.

Data analysis and statistics. Traces were recorded on a 64-bit computer using LabChart 7 Pro (ADInstruments). The airflow signal was high-pass filtered (>0.1 Hz) to eliminate DC shifts and slow drifts, and used to calculate respiratory frequency, period, inspiratory (T_I) and expiratory (T_E) durations. The airflow signal was integrated to compute tidal volume (V_T).

Cell counts were performed on three sequential sagittal sections as defined by the localization of *Sst*-immunoreactive neurons and soma distances relative to the caudal boundary of the facial motor nucleus were calculated. Counts were performed with ImageJ (http://rsb.info.nih.gov/ij/) and exported to Igor (Wavemetrics) for analysis with custom software.

All statistics were performed in Igor (Wavemetrics). Statistical significance was set at $P < 0.05$. One-way ANOVAs and pairwise comparisons using Tukey's HSD test were performed for all experiments except in **Figure 5b**, where an unpaired *t* test was used. All values are presented as mean ± s.e.m. No statistical methods were used a priori to pre-determine sample sizes, but our sample sizes are similar to those reported in previous publications[1,41]. Data distribution was assumed to be normal, but this was not formally tested.

Phase response analysis. The photostimulation-evoked reset of the respiratory rhythm was studied by applying a single 100-ms light pulse at various times

during the respiratory cycle. The respiratory phase in each photostimulation or photoinhibition breath was based on the prior (control) respiratory period and defined as spanning 0–360°. Across experiments, inspiration (defined as the period of inward airflow) lasted from onset at 0° until 71.8 ± 11.6° ($n = 5$) in ChR2 experiments and until 77.9 ± 7.1° ($n = 7$) for Arch experiments; expiration was defined as the remainder of the cycle. Thus, the phase of any event could be calculated based on the time at which it occurred relative to the preceding inspiratory onset and referenced to the preceding control period. More specifically, phase values were obtained by calculating the ratio of the event onset time to the respiratory period and multiplying by 360°.

Stimulus phase (ϕ_{stim}), induced phase (ϕ_i), and expected phase (ϕ_e) of the respiratory cycle were computed (see **Fig. 2a**)[38,42] and plotted using software written in Igor (Wavemetrics). ϕ_{stim}, that is, the time of laser onset relative to the ongoing respiratory cycle, was defined as the delay from the beginning of the previous inspiration to the time of laser onset. ϕ_e represents the total respiratory period, defined using the previous cycle as a control. ϕ_i is the respiratory period during the light-affected cycle. The difference between ϕ_i and ϕ_e was the net phase shift (ϕ_{shift}). If the light had no effect, $\phi_e = \phi_i$, and $\phi_{shift} = 0$.

A **Supplementary Methods Checklist** is available.

35. Adamantidis, A.R., Zhang, F., Aravanis, A.M., Deisseroth, K. & de Lecea, L. Neural substrates of awakening probed with optogenetic control of hypocretin neurons. *Nature* **450**, 420–424 (2007).
36. Gradinaru, V. *et al.* Targeting and readout strategies for fast optical neural control *in vitro* and *in vivo*. *J. Neurosci.* **27**, 14231–14238 (2007).
37. Paxinos, G., Franklin, K.B.J. & Franklin, K.B.J. *The Mouse Brain in Stereotaxic Coordinates* (Academic Press, 2001).
38. Pagliardini, S. *et al.* Active expiration induced by excitation of ventral medulla in adult anesthetized rats. *J. Neurosci.* **31**, 2895–2905 (2011).
39. Poyatos, I., Ponce, J., Aragon, C., Gimenez, C. & Zafra, F. The glycine transporter GLYT2 is a reliable marker for glycine-immunoreactive neurons. *Brain Res. Mol. Brain Res.* **49**, 63–70 (1997).
40. Zeilhofer, H.U. *et al.* Glycinergic neurons expressing enhanced green fluorescent protein in bacterial artificial chromosome transgenic mice. *J. Comp. Neurol.* **482**, 123–141 (2005).
41. McKay, L.C., Janczewski, W.A. & Feldman, J.L. Sleep-disordered breathing after targeted ablation of preBotzinger complex neurons. *Nat. Neurosci.* **8**, 1142–1144 (2005).
42. Lewis, J., Bachoo, M., Polosa, C. & Glass, L. The effects of superior laryngeal nerve stimulation on the respiratory rhythm: phase-resetting and aftereffects. *Brain Res.* **517**, 44–50 (1990).